AAS 08-207

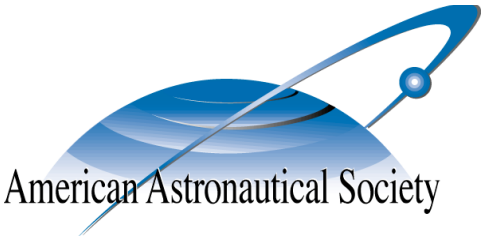

American Institute of
Aeronautics and Astronautics

OPEN-LOOP ELECTROSTATIC SPACECRAFT COLLISION AVOIDANCE USING PATCHED CONICS ANALYSIS

Shuquan Wang and Hanspeter Schaub

AAS/AIAA Spaceflight Mechanics Meeting

Galveston, Texas **January 27-31, 2008**

AAS Publications Office, P.O. Box 28130, San Diego, CA 92198

AAS 08-207

OPEN-LOOP ELECTROSTATIC SPACECRAFT COLLISION AVOIDANCE USING PATCHED CONICS ANALYSIS

Shuquan Wang* **and Hanspeter Schaub†**

Collision avoidance is becoming a key concern with many envisioned spacecraft cluster mission concepts. This paper considers a 2-spacecraft collision avoidance problem where the craft are floating a few dozen meters apart and slowly drifting towards each other. The Coulomb thrusting approach is used to develop a trajectory programming strategy to avoid the potential collision while conserving the initial relative velocity direction and magnitude. By assuming the spacecraft to be floating freely in deep space and maintaining piece-wise constant electrostatic charge levels, the relative trajectory are described through splices of conic sections. A symmetric 3-conic-section trajectory programming strategy is designed to match up the arrival direction with the departure direction. Allowing general conic sections while orbiting each other, five constraints are introduced to formulate the five degrees of freedom (DOF) problem. Newton's method is used to iterate across one variable to determine an answer A special circular circumnavigation case is also discussed which provides an easy to determine solution.

INTRODUCTION

Spacecraft collision avoidance is an important topic in close formations and small satellite swarms with separation distances ranging on the order of dozens to hundreds of meters. A collaborative formation or swarm of multiple satellites flying closely has many advantages over a single large monolithic satellite. However, spacecraft swarm concepts also introduce the issue of potential collisions due to the failure of the control or the sensor of some spacecraft within the cluster, or the lack of the guidance strategy to guarantee collision avoidance.

Many previous works in spacecraft collision avoidance consider specifically the probability of the collision for satellites in a formation, and determines the spacecraft maneuvers to lower the collision risk to an acceptable level. Russell P. Patera and Glenn E. Peterson in Reference 1 develop a method to select a maneuver that will reduce the collision probability. The method minimizes the maneuver magnitude and space vehicle propellant expenses. G. L. Slater et al. in Reference 2 use the available state and disturbance information to calculate the actual probability of collision based on a probabilistic model, and then discusses the velocity correction requirements to avoid collisions. In Reference 3, Russell P. Patera proposes a spherical conflict volume to calculate the conflict probability in identifying high-risk conjunctions. The conflict probabilities are larger than associated collision probabilities and therefore are more easily interpreted.

This paper discusses an active avoidance scenario when a potential collision has been detected to happen. Not focusing on reducing the probability of a collision or a confliction, the paper is going to design an immediate control using only electrostatic (Coulomb) forces to prevent the collision. Note

*Graduate Research Assistant, Aerospace Engineering Sciences Department, University of Colorado, Boulder, CO.

†Associate Professor, H. Joseph Smead Fellow, Aerospace Engineering Sciences Department, University of Colorado, Boulder, CO.

that most of the previous works in spacecraft collision avoidance are based on the control strategies' capability to control all three components of the thrust vector in 3-D space. These control strategies use propellent, which will increase the fuel budget of the spacecraft. Further, the associated exhaust plume impingement may cause damage to instruments on board when spacecraft are flying less than 100 meters apart. Coulomb force has advantages over traditional thrusters in preventing a spacecraft collision in that it is essentially propellentless and will not increase the fuel budget. Thus it will not generate any propellent plume impingement issues that threaten neighboring spacecraft.

The application of Coulomb force in spacecraft cluster flying has sprung out a lot of discussions since Lyon B. King et al. originally introduced Coulomb Formation Flying (CFF) in Reference 4. CFF uses Coulomb forces to control the distances between spacecraft to achieve the desired relative motion. Spacecraft will naturally charge to either positive or negative voltages due to their interaction with the local space plasma environment. The spacecraft charge level can be actively controlled by continuously emitting electrons or ions. The fuel-efficiency of Coulomb thrusting is at least 3–5 orders greater than that of Electric Propulsion (EP).[4] Coulomb thrusting typically requires only a few Watts of electrical power to operate.[4] A challenge of CFF is that, unlike conventional thrusters that can produce a thrust vector in any direction, the Coulomb forces only lie along the line-of-sight directions between spacecraft. But this is less of an issue in using Coulomb forces to avoid a collision. The most important factor in preventing collision is the separation distance, which can be fully controlled using Coulomb forces. Another challenge of CFF is that the sparse space plasma will shield electrostatic charges. This effect will reduce the amount of electrostatic force that a neighboring charged spacecraft will experience. The amount of shielding is characterized by the Debye length[5].[6] At separation distances greater than a Debye length the perceived inter-craft Coulomb force quickly becomes negligle. At LEO where the plasma is relatively dense and cold, the Debye length is on the order of centimeters. This results in a strong shielding of Coulomb forces and makes Coulomb thrusting un-feasible. However, at GEO the Debye lengths range between 100–1000 meters.[4,7] At 1 AU in deep space the Debye length ranges around 20–50 meters.[4] This makes the Coulomb thrusting concept feasible for HEO and deep space missions while the minimum separation distances are less than 100 meters.

The CFF concept has been investigate for several different mission scenarios in recent publications V. Lappas et al. in Reference 8 develops a hybrid propulsion strategy by combining Coulomb forces and standard electric thrusters for formation flying on the orders of tens of meters in GEO. Reference 9 analyses the stability of a spinning 2-craft Coulomb tether. It shows that if the Debye length is larger than the separation distance, the nonlinear radial motion is locally stable, otherwise unstable. And the perturbed out-of-plane motion is always stable regardless of Debye length. H. Vasavada and H. Schaub in Reference 10 present analytical tools to determine the charge solution for a static 4–craft formation. Reference 11 designs a two-stage charge feedback control strategy for a 1–D constrained Coulomb structure. It also analyses the condition for symmetric relative motions of Coulomb structure to be stabilizable by investigating the total energy of the system. I. I. Hussein and H. Schaub derive the collinear three-craft spinning family of solutions in Reference 12. A feedback control based on the linearized model is designed to stabilize a symmetric Coulomb tether system. Asymptotic stability is achieved if the system's angular momentum is equivalent to that of the desired equilibrium. However, none of these CFF related works consider the issue of performing active collision avoidance. Such a capability will be required when considering flying larger numbers of craft in close proximity.

The previous charged collision avoidance work in Reference 13 develops a collision avoidance

strategy using an active charge control law with separation distance and rate feedback. The controller is designed based on Lyapunov stability analysis. Without charge saturations the controller can prevent any collision. Considering charge saturations, the paper finds the analytical criteria for an avoidable collision by assuming the Debye length to be infinity. Numerical simulations show that the criteria is usable even when limited Debye length is applied on spacecraft. While this feedback control strategy can maintain specified safety separation distances, this control will cause the craft to depart in a different direction from when the collision avoidance maneuver started.

This paper investigates using Coulomb forces to prevent a potential collision between two slowly approaching spacecraft. The feasible electrostatic forces are typically too small to avoid the collision of two rapidly approaching spacecraft. A new open-loop control approach to prevent the collision is presented which aims to maintain the initial velocity vector magnitudes and directions of the approaching craft. By assuming the Debye length to be large compared to the separation distance, and that the spacecraft charges are constant, the relative EOM has exactly the same form as gravitational two body problem (G2BP). Thus the relative trajectory of the spacecraft is a conic section.[14] Through switching the value of the spacecraft charges, a patched conic section trajectory is investigated which will satisfy the separation distance and the departure velocity requirements. Numerical simulation will illustrate how these open-loop charge solutions will generate the desired collision avoidance maneuver.

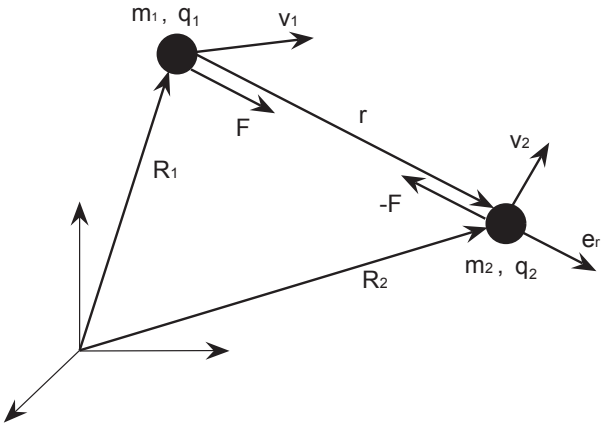

Figure 1 Illustration of the 2-spacecraft system.

CHARGED SPACECRAFT EQUATIONS OF MOTION

Consider two spacecraft free-flying in 3-dimensional space where there are no external forces acting on the system. The scenario of the two body system is shown in Figure 1. The Coulomb force vector between the two spacecraft, acting on m_1, is

$$\boldsymbol{F} = -k_c \frac{q_1 q_2}{r^3} e^{-\frac{r}{\lambda_d}} \boldsymbol{r} = -k_c \frac{q_1 q_2}{r^2} e^{-\frac{r}{\lambda_d}} \hat{\boldsymbol{e}}_r \tag{1}$$

Here the parameter $k_c = 8.99 \times 10^9 \mathrm{C}^{-2} \cdot \mathrm{N} \cdot \mathrm{m}^2$ is the Coulomb constant, r is the separation distance between the two spacecraft, $\boldsymbol{r}$ is the relative position vector pointing from spacecraft 1 (SC1) to spacecraft 2 (SC2), $\hat{\boldsymbol{e}}_r$ is the unit vector of $\boldsymbol{r}$, and λ_d is the Debye length. The smaller the plasma Debye length is, the shorter the effective range is of a given electrical charge. For high

Earth orbits the Debye length ranges between 100–1000 meters.[4,15,7] CFF typically has spacecraft separation distances ranging up to 100 meters.

The inertial equations of motion of the two charged spacecraft are approximated through the point-charge models using

$$m_1\ddot{\boldsymbol{R}}_1 = -k_c\frac{q_1q_2}{r^2}e^{-\frac{r}{\lambda_d}}\hat{\boldsymbol{e}}_r \tag{2a}$$

$$m_2\ddot{\boldsymbol{R}}_2 = k_c\frac{q_1q_2}{r^2}e^{-\frac{r}{\lambda_d}}\hat{\boldsymbol{e}}_r \tag{2b}$$

where $\boldsymbol{R}_i$ is the inertial position vector of the i^{th} spacecraft. The inertial relative acceleration vector $\ddot{\boldsymbol{r}}$ is

$$\ddot{\boldsymbol{r}} = \ddot{\boldsymbol{R}}_2 - \ddot{\boldsymbol{R}}_1 = \frac{k_cq_1q_2}{m_1m_2r^2}(m_1+m_2)e^{-\frac{r}{\lambda_d}}\hat{\boldsymbol{e}}_r \tag{3}$$

Note that these equations do not explicitly consider orbital motion of spacecraft. However, if the collision avoidance maneuver time is very small compared to the cluster orbital period, then they can also be considered an approximation of the charged relative orbital motion. For example, a GEO spacecraft collision avoidance maneuver which takes minutes would be very short compared to the 1 day orbit period, and thus the relative orbital motion would have a secondary effect on the relative motion.

This paper is going to find a symmetric patched conic section trajectory to prevent a collision, while forcing the departure velocity vector to be the same as the initial arrival velocity vector. Reference 14 shows that if $\lambda_d \to \infty$, and the charge product $Q = q_1q_2$ is constant, then the relative motion trajectory of the two spacecraft is a conic section. Letting $\lambda \to \infty$ and defining $\mu = -k_c\frac{Q(m_1+m_2)}{m_1m_2}$, Eq. (3) can be rewritten as

$$\ddot{\boldsymbol{r}} = -\frac{\mu}{r^3}\boldsymbol{r} \tag{4}$$

Eq. (4) has exactly the same algebraic form as the EOM of G2BP. If the charge product Q is constant, then the effective gravitational coefficient μ is also constant. Thus the resulting motion can be described by a conic section. Note that here μ can be positive or negative. For the oppostive charge sign case $Q < 0$, resulting in a positive effective gravitational constant $\mu > 0$. In this case Eq. (4) is exactly the same as the G2BP. If $Q > 0$ and $\mu < 0$, then the relative trajectory is a repulsive hyperbola, where SC2 is moving along a hyperbola, and SC1 stays at the farther focus point.[14]

Thus to find a symmetric patched conic section trajectory, this paper assumes that the two spacecraft are flying in free space without external forces, and the Debye length is approximated to be infinityly large compared to the separation distance.

SYMMETRIC TRAJECTORY PROGRAMMING STRATEGY

This section develops a numerical routine used to find a symmetric solution of the relative trajectory satisfying certain collision avoidance constraints. An example of the symmetric relative trajectory scenario is shown in Figure 2. At the beginning, the two spacecraft are flying freely and approaching each other such that their minimum separation distance will violate a desired safety distance. At the point A, the separation distance between the spacecraft reaches a potential collision region range r_o. The spacecraft are charged such that $Q > 0$, thus the spacecraft start to repel each

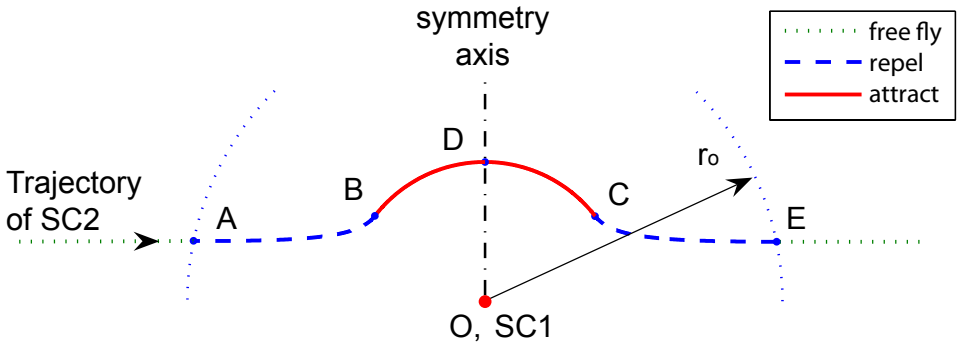

Figure 2 Illustration of the symmetric patched conic section relative motion trajectory with respect to mass m_1.

other to avoid the collision. Before arriving at the point B, the magnitude of the charge product is held constant. Thus the arc $\widehat{AB}$ is a repulsive hyperbola. At the point B the charge product switches to a negative value such that the spacecraft are attracting each other. From the point B to the point C, the charge product is again held constant. The arc $\widehat{BC}$ is an attractive conic section which can be ellipsis, parabola, or hyperbola depending on the relative arrival velocity magnitude. At the point C the charge product switches back to the same value as in arc $\widehat{AB}$ to produce a symmetric trajectory to $\widehat{AB}$. At the point E, the charges are turned off and the spacecraft begin to fly freely in space.

The relative trajectory in Figure 2 is symmetric about the $\overline{OD}$ axis. This symmetry axis is perpendicular to the initial relative velocity and acrosses the spacecraft m_1 point O. At the beginning, the two spacecraft are flying without Coulomb forces. When the distance decreases to a certain prescribed value r_o at point A, the two spacecraft begin to repel each other. At point B, the craft turn to attract each other. Point C is the corresponding symmetric point of B, and E corresponds to A. At point C, the spacecraft begin to repel each other, and at point E the control charges are turned off and the spacecraft begin to fly freely. For the convenience of describing the process, denote the arc $\widehat{AB}$ as "Phase I", $\widehat{BC}$ as "Phase II" and $\widehat{CE}$ as "Phase III".

Constraints

In this scenario, there are five unknowns that need to be determined: three charge products Q_{I}, Q_{II} and Q_{III}, and two times at points B and C. Generally there are an infinity of possible charge and charge switching time solutions which achieve a successful collision avoidance. This section introduces constraints which guarantee a desired minimum separation distance r_s, as well conditions which will match the arrival and departure velocity vector magnitudes and direction. Further, as the craft depart it is desirable to have the craft follow their original trajectories to cause minimal disruption to the overall formation motion.

The collision avoidance task requires that the separation distance $r(t)$ must be greater than a certain safe-restraint distance r_s for all time:

$$r(t) \geq r_s \tag{5}$$

This constraint is global and comes from the collision avoidance mission. To find a symmetric trajectory solution as shown by Figure 2, more information must be extracted. For the arc $\widehat{AB}$ and

$\widehat{CE}$ to be symmetric, the first and final set of charge products should be equal, that is

$$Q_{\mathrm{I}} = Q_{\mathrm{III}} \tag{6}$$

For the arc $\widehat{BC}$ in Phase II to be symmetric about the symmetric axis $\overline{OD}$, the point D must be the periapsis or apoapsis of Phase II, unless the arc $\widehat{BC}$ is a part of a circular orbit. This requirement is formulated as:

$$r_D = r_{p\mathrm{II}}, \quad \text{or} \quad r_D = r_{a\mathrm{II}} \tag{7}$$

Another requirement for Phase II to be symmetric is that the point C should be the mirror image of the point B. This can be described by the geometry relation

$$\angle BOD = \angle COD \tag{8}$$

So far three equality constraints, Eqs. (6), (7) and (8), and one inequality constraint in Eq. (5) are presented to narrow down the trajectory programming problem. The three equality constraints decrease the system's degrees of freedom (DOF) to be two. Two more equality constraints are required to develop an iteration loop.

The charge products of Phase I and III can be written as

$$Q_{\mathrm{I}} = Q_{\mathrm{III}} = \alpha Q_{\max} \tag{9}$$

where $0 < \alpha \leq 1$ and $Q_{\max} > 0$ is the maximum charge product of the two spacecraft. Phase I is designed to be a concave curve in order to stop the approaching of the spacecraft. Thus the main purpose of Phase I is to prevent collision. Because larger charge product prevents a collision more quickly, it's resonable to choose $\alpha = 1$ such that

$$Q_{\mathrm{I,\,III}} = Q_{\max} \tag{10}$$

The inequality constraint in Eq. (5) can be written as:

$$r_{\min} = \gamma r_s \tag{11}$$

here $\gamma \geq 1$. In the iteration search routine, the parameter γ can be chosen to be a fixed value greater than 1.

Now there are five equality constraints to solve the patched conic collision avoidance trajectory. Eqs. (6) – (8) are from the symmetric patched conic section properties. The constraint given by Eq. (11) is required by the collision avoidance task. And the last constraint in Eq. (10) is chosen to achieve a quick collision avoidance.

Numerical Iteration Routine

This section develops a numerical iteration routine to find a symmetric patched conic section trajectory for the collision avoidance problem. The charge product Q_{I} and the initial conditions $[\boldsymbol{r}_A, \dot{\boldsymbol{r}}_A]$ determine the conic section of Phase I. Without loss of generality, assume that $t_A = 0$. If t_B is given, the angle $\angle AOB$ can be calculated using Kepler's equation in Phase I. The states

$[\boldsymbol{r}_B, \dot{r}_B]$ are also determined by solving the orbit EOM of Phase I. Utilizing the constraint that the point D must be the periapsis or apoapsis of Phase II, the point C can be determined by the constraint in Eq. (8). Phase III is determined by the state of point C, which can be infered from t_B. Thus the charge switching time variable t_B logically determines the whole patched conic section trajectory. In the iteration routine, t_B is chosen as the variable to be propagated.

The algorithm assumes that the relative position vector $\boldsymbol{r}_A$ and the relative velocity $\dot{\boldsymbol{r}}_A$ at point A can be measured. The conic section properties of Phase I can be completely solved using $\boldsymbol{r}_A$ and $\dot{\boldsymbol{r}}_A$. The eccentricity vector of Phase I is

$$\boldsymbol{c}_{\mathrm{I}} = \dot{\boldsymbol{r}}_A \times \boldsymbol{h} - \frac{\mu_{\mathrm{I}}}{r_A}\boldsymbol{r}_A \tag{12}$$

where $\boldsymbol{h} = \boldsymbol{r}_A \times \dot{\boldsymbol{r}}_A$ is the specific angular momentum of the system, and

$$\mu_{\mathrm{I}} = -k_c \frac{Q_{max}(m_1 + m_2)}{m_1 m_2} \tag{13}$$

is the effective gravitational coefficient of Phase I. Further, note the notation $r_A = |\boldsymbol{r}_A|$. The vector $\boldsymbol{h}$ is constant by the assumption that there are no external forces acting on the sytem. The eccentricity and semi-major axis of Phase I are calculated by

$$e_{\mathrm{I}} = -\frac{\|\boldsymbol{c}_{\mathrm{I}}\|}{\mu_{\mathrm{I}}} \tag{14a}$$

$$a_{\mathrm{I}} = \frac{r_A \mu_{\mathrm{I}}}{2\mu_{\mathrm{I}} - r_A v_A^2} \tag{14b}$$

where $v_A = \|\dot{\boldsymbol{r}}_A\|$ is the magnitude of the relative velocity vector. The angle $\angle AOD$ is calculated as

$$\angle AOD = \arctan\left(\frac{h}{r_A v_A}\right) - \frac{\pi}{2} \tag{15}$$

Because t_B has been chosen as the variable to be propagated in the iteration loop, it starts from an initial guess value, and is updated using an error of a target function. In the present formulation of the algorithm the time point t_B is assumed to be given. The states at point B can be determined by using the conic section properties of Phase I. The mean hyperbolic anomaly of point B considered in Phase I is calculated using the Kepler's equation:

$$N_{B\mathrm{I}} = N_{A\mathrm{I}} + \sqrt{\frac{\mu_{\mathrm{I}}}{a_{\mathrm{I}}^3}} \cdot t_B = N_{A\mathrm{I}} + n_{\mathrm{I}} \cdot t_B \tag{16}$$

Then the hyperbolic anomaly $H_{B\mathrm{I}}$ is calculated by numerically solving the standard anomaly relationship:[16]

$$N_{B\mathrm{I}} = e_{\mathrm{I}} \sinh(H_{B\mathrm{I}}) + H_{B\mathrm{I}} \tag{17}$$

Thus the true anomaly of point B is determined by

$$f_{B\mathrm{I}} = 2 \cdot \arctan\left(\tanh\left(\frac{H_{B\mathrm{I}}}{2}\right)\sqrt{\frac{e_{\mathrm{I}}+1}{e_{\mathrm{I}}-1}}\right) \tag{18}$$

The radius and the magnitude of the relative velocity at point B are

$$r_B = \frac{h^2/\mu_{\mathrm{I}}}{1 - e_{\mathrm{I}} \cos f_{B\mathrm{I}}} \tag{19a}$$

$$v_B = \sqrt{\mu_{\mathrm{I}} \left(\frac{2}{r_B} - \frac{1}{a_{\mathrm{I}}} \right)} \tag{19b}$$

here h is the magnitude of the specific angular momentum determined by initial conditions. Eq. (19b) is from the energy equation.

After obtaining the relative motion states at point B, Phase II can be determined by the symmetric conic section constraints. Specifically, the charge product Q_{II} and point C can be calculated. At first, the angle $\angle AOB$ is calculated by

$$\angle AOB = |f_{B\mathrm{I}} - f_{A\mathrm{I}}| \tag{20}$$

The angle $\angle BOD$ is determined by the geometry relation:

$$\angle BOD = \angle AOD - \angle AOB \tag{21}$$

According to the symmetric constraint in Eq. (8), the angle

$$\angle COD = \angle BOD \tag{22}$$

is determined. Thus the point C is located. Note that of the five variables which determine the symmetric conic section trajectory, the points B, C, the charge products Q_{I}, Q_{III} have been solved. The only variable left to be determined is the charge product Q_{II}. From the definition of μ in Eq. (4) we find:

$$\mu_{\mathrm{II}} = -k_c \frac{Q_{\mathrm{II}}(m_1 + m_2)}{m_1 m_2} \tag{23}$$

Once μ_{II} is solved, Q_{II} is also determined. The following development is going to solve for μ_{II} based on the states of the point B and the symmetric constraints.

Since the arc $\widehat{BC}$ is a part of a conic section, it has all of the properties of conic section orbit. The semi latus rectum can be expressed in two ways:

$$p = a(1 - e^2) = \frac{h^2}{\mu} \tag{24}$$

Solving for the eccentricity e, yields

$$e = \sqrt{1 - \frac{h^2}{\mu a}} \tag{25}$$

From the energy equation, the term $\frac{1}{\mu a}$ is expressed as:

$$\frac{1}{\mu a} = -\frac{v^2}{\mu} + \frac{2}{r} \tag{26}$$

Substituting Eq. (26) into Eq. (25), yields

$$e = \sqrt{1 + \left(\frac{v^2}{\mu} - \frac{2}{r}\right)\frac{h^2}{\mu}} \tag{27}$$

For a given two body system without external forces, the specific angular momentum h is constant. Thus the expression of the eccentricity in Eq. (27) contains only three variables r, v and μ. Substituting Eq. (27) into the radius equation, yields

$$\begin{aligned} r &= \frac{h^2/\mu}{1 + e\cos f} \\ &= \frac{h^2}{\mu + \cos f\sqrt{\mu^2 + \left(v^2 - \frac{2\mu}{r}\right)h^2}} \end{aligned} \tag{28}$$

Transforming Eq. (28) to separate the square root term, yields

$$\cos f\sqrt{\mu^2 + \left(v^2 - \frac{2\mu}{r}\right)h^2} = \frac{h^2}{r} - \mu \tag{29}$$

Squaring Eq. (29) and grouping terms of μ yields

$$(\cos^2 f - 1)\mu^2 + \frac{2h^2}{r}(1 - \cos^2 f)\mu + \cos^2 f v^2 h^2 - \frac{h^4}{r^2} = 0 \tag{30}$$

Because $1 - \cos^2 f = \sin^2 f$, Eq. (30) can be further simplified to

$$\sin^2 f\mu^2 - \frac{2h^2}{r}\sin^2 f\mu - \cos^2 f v^2 h^2 + \frac{h^4}{r^2} = 0 \tag{31}$$

With h being constant, this quadratic equation of μ contains the variables f, r and v. Note that Eq. (31) is valid for all conic section orbits. To solve for μ_{II}, evaluate f, r and v at point B in Phase II and then solve the following quadratic equation

$$\sin^2 f_{B\text{II}}\mu_{\text{II}}^2 - \frac{2h^2}{r_B}\sin^2 f_{B\text{II}}\mu_{\text{II}} - \cos^2 f_{B\text{II}}v_B^2 h^2 + \frac{h^4}{r_B^2} = 0 \tag{32}$$

where r_B and v_B are given by Eq. (19). If the point D is the periapsis location,then

$$f_{B\text{II}} = -\angle BOD \tag{33}$$

Else, if D is the apoapsis location, then

$$f_{B\text{II}} = \pi - \angle BOD \tag{34}$$

In both cases, the resulting final equations after substituting $f_{B\text{II}}$ into Eq. (32) are identical:

$$\underbrace{\sin^2\angle BOD}_{l_1}\mu_{\text{II}}^2 \underbrace{-\frac{2h^2}{r_B}\sin^2\angle BOD}_{l_2}\mu_{\text{II}} \underbrace{-\cos^2\angle BOD v_B^2 h^2 + \frac{h^4}{r_B^2}}_{l3} = 0 \tag{35}$$

Analytically solving for μ_{II} from Eq. (35), the charge product in Phase II is obtained by Eq. (23).

Note that generally there are two solutions of μ_{II} to Eq. (35). One of them corresponds to the case that D is the apoasis of the arc $\widehat{BC}$, the other one corresponds to the case that D is the periapsis. The completed paper will analyse this phenomenon.

The previous development outlines the formulas used to solve the points B and C, and the charge product of Phase II Q_{II} assuming the variable t_B is given. However, in our present collision avoidance application t_B is not explicity determined. Note that four constraints have been used in deriving those formulas, Eqs. (6), (7), (8) and (10). The constraint in Eq. (11) hasn't been utilized. The numerical search routine is intended to find an appropriate t_B such that the closest distance $r_{\text{min}} = \gamma r_s$, where $\gamma \geq 1$.

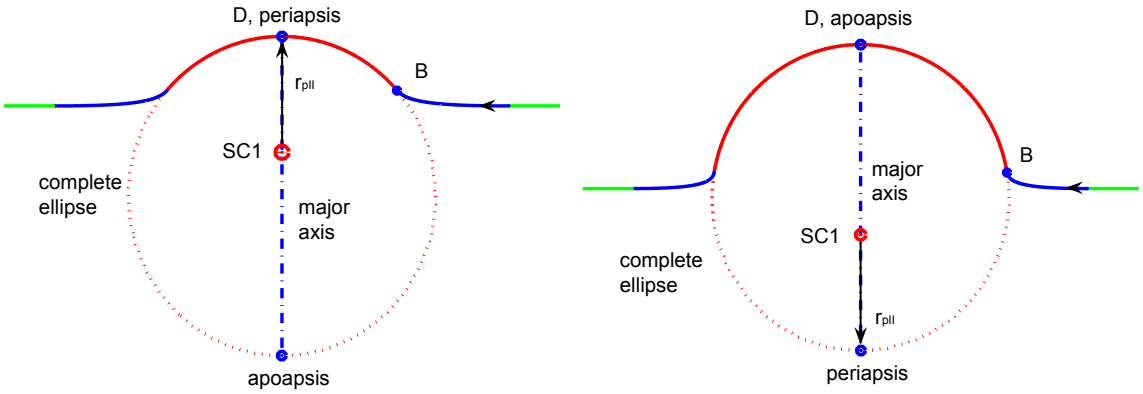

(a) point D is the periapsis of Phase II.

(b) point D is the apoapsis of Phase II.

Figure 3 Illustration of two cases of point D.

If the point D is the periapsis of Phase II, then r_D is the closest distance in Phase II. And the distance in Phase I and Phase III are greater than or equal to r_B, and $r_B > r_D$ because the point B is on Phase II, thus in this case $r_{\text{min}} = r_D = r_{p\text{II}}$. This scenario is shown in Figure 3(a). When the piont D is the apoapsis of Phase II, the scenario is shown in Figure 3(b). The closest distance changes to be $r_{\text{min}} = r_B$ because $r_B < r_D$. But in this case r_B is difficult to calculate because the formulas for solving this general point is complicated. To simplify the calculations, the criteria for the convergence is modified to be

$$r_{p\text{II}} = \gamma r_s \tag{36}$$

Note that this criteria is more conservative than $r_{\text{min}} = \gamma r_s$. When $r_D = r_{p\text{II}}$, $r_{p\text{II}} = \gamma r_s$ is equavilent to $r_{\text{min}} = \gamma r_s$. If $r_D = r_{a\text{II}}$, $r_{\text{min}} > r_{p\text{II}} = \gamma r_s$. Define the target function as:

$$g(t_B) = r_{p\text{II}}(t_B) - \gamma r_s \tag{37}$$

Newton's method is used to find t_B that satisfies $g(t_B) = 0$. The iteration algorithm propagates according to the following steps:

Step 1 *Initialization:* From the measurements $\boldsymbol{r}_A$ and $\dot{\boldsymbol{r}}_A$, calculate e_I, a_I through Eq. (14), and calculate the angle $\angle AOD$ through Eq. (15). Initiate $t_B = t_B^{(0)}$.

The initial guess $t_B^{(0)}$ can be chosen as the time for SC2 to fly from the point A to the periapsis of Phase I:

$$t_B^{(0)} = \frac{|N_A|}{\sqrt{\mu_{\rm I}/a_{\rm I}^3}} \tag{38}$$

Step 2 Solve for the point B's states r_B and v_B through Eqs. (16)–(19).

Step 3 Solve for $\mu_{\rm II}$ by Eq. (35). Calculate $r_{p\rm II}$ through

$$r_{p\rm II} = a_{\rm II}(1 - e_{\rm II}) \tag{39}$$

and $a_{\rm II}$ is solved by the energy equation, $e_{\rm II}$ is calculated through Eq. (27) evaluating at point B in Phase II.

Step 4 Find $g' = \frac{\partial g}{\partial t_B}$ using the finite difference method.

Step 5 Update $t_B^{(i+1)} = t_B^{(i)} - \frac{g}{g'}$, $i = i + 1$.

Step 6 Judge whether $|g(t_B)| <$ Tol. If yes, $t_B = t_B^{(i)}$, **STOP**. Otherwise, go to **Step 2**.

CIRCULAR TRANSITIONAL ORBIT PROGRAMMING

A special case of the symmetric trajectory case is that the Phase II trajectory is a section of a circle. Because the circular orbit is a special case of the elliptic orbit it provides an additional constraint to determine the collision avoidance maneuver. With the previous initial conditions at the point A we assumed that $Q_{\rm I} = Q_{\rm III} = Q_{\max}$. As a result the parameters t_B and $\mu_{\rm II}$ are determined by specifying a symmetric trajectory of Phase II satisfying the safety constraint $r_{p\rm II} = \gamma r_s$. However, this leads to an infinity of possible answers. Depending on the initial conditions of the numerical iteration routine, the iterations may not converge to a real or practical answer.

This section investigates the circular Phase II trajectory special case. Through the initial conditions at the point A a unique set of variables $(Q_{\rm I}, t_B, \mu_{\rm II})$ are found such that Phase II is a part of a circular orbit, and also satisfies the safety constraint $r_B = \gamma r_s$ (the point B is the start point of the circular trajectory). In this scenario the Phase I charge product Q_I is not set to $Q_{\max}$, but it is determined through the desired circular collision avoidance geometry. Note that for Phase II to be part of a circle, the relative velocity at the point B must be perpendicular to the relative position vector, thus the point B must be the periapsis of Phase I. The switching time variable t_B is calculated through

$$t_B = \frac{|N_{A\rm I}|}{\sqrt{\mu_{\rm I}/a_{\rm I}}} \tag{40}$$

with the right hand side of this equation is completely determined by $\mu_{\rm I}$, which in return is is determined by $Q_{\rm I}$. Thus, once $Q_{\rm I}$ is found, the shape of Phase I and the point B are all determined.

The safety constraint to avoid a collision is expressed by the condition $r_B = \gamma r_s$. The radius r_B is calculated by

$$r_B = \frac{h^2/\mu_{\rm I}}{1 - e_{\rm I}} \tag{41}$$

where the eccentricity e_{I} is determined through the eccentricity vector as

$$e_{\mathrm{I}} = -\frac{\|\boldsymbol{c}_{\mathrm{I}}\|}{\mu_{\mathrm{I}}} = \left\| \frac{\dot{\boldsymbol{r}}_A \times \boldsymbol{h}}{\mu_{\mathrm{I}}} - \frac{\boldsymbol{r}_A}{r_A} \right\| \tag{42}$$

Thus the constraint for a circular Phase II trajectory is

$$\frac{h^2/\mu_{\mathrm{I}}}{1 - e_{\mathrm{I}}} = \gamma r_s \tag{43}$$

Note that the left hand side of Eq. (43) is a function of μ_{I}. Analytically solving for μ_{I} is too complex. Instead, to numerically solve Eq. (43) we define the target function:

$$g_2(\mu_{\mathrm{I}}) = \gamma r_s - r_B = \gamma r_s - \frac{h^2/\mu_{\mathrm{I}}}{1 - e_{\mathrm{I}}} \tag{44}$$

The purpose of the numerical method is to find a proper μ_{I} to make $g_2 = 0$. A solution indicates that the safety constraint is satisfied and that the 2 spacecraft will orbit each other on a circular arc of radius γr_s during Phase II. The Newton-Raphson's method is employed to solve the equation $g_2 = 0$ in this paper.

After obtaining μ_{I} through solving $g_2 = 0$, the variable t_B is determined by Eq. (40). These values of μ_{I} and t_B ensure that at the point B the relative speed vector is perpendicular to the relative position vector, and the radius $r_B = \gamma r_s$. The next step is to find a proper μ_{II} that results in a circular orbit. Using the momentum magnitude expression of a circular orbit, μ_{II} is found to be

$$\mu_{\mathrm{II}} = \frac{h^2}{r_{\mathrm{II}}} = \frac{h^2}{r_B} \tag{45}$$

To find the Phase II duration time t_{II}, the Phase II symmetry constraint is utilized. Note that the angular velocity is constant in Phase II, the duration time is proportional to the angle $\angle BOC$:

$$t_{\mathrm{II}} = \angle BOC \cdot \frac{T_{\mathrm{II}}}{2\pi} = 2\angle BOD \cdot \frac{T_{\mathrm{II}}}{2\pi} = \frac{\angle BOD \cdot T_{\mathrm{II}}}{\pi} \tag{46}$$

The period of the Phase II circular orbit is $T_{\mathrm{II}} = \sqrt{\mu_{\mathrm{II}}/r_B^3}$, while the angle $\angle BOD$ is given by

$$\angle BOD = \angle AOD - |f_{A\mathrm{I}}| \tag{47}$$

and the angle $\angle AOD$ is expressed in Eq. (15).

Thus a symmetric trajectory with Phase II being a part of a circular orbit has been found. Figure 4 shows the scenario of the trajectory. Future work may be engaged to find a more optimal solution that results in minimum charge or energy expenses.

NUMERICAL SIMULATIONS

A numerical iteration routine using Newton's method to solve for a symmetric patched conic section trajectory has been set up. The routine is designed to search for an appropriate time value t_B for SC2 passing by the point B, such that the target function $g(t_B)$ defined in Eq. (37) converges to zero. Once $g(t_B)$ converges to zero, then $r_{p\mathrm{II}} = \gamma r_s$ where $\gamma \geq 1$. the collision avoidance requirement $r_{\min} \geq r_s$ is satisfied.

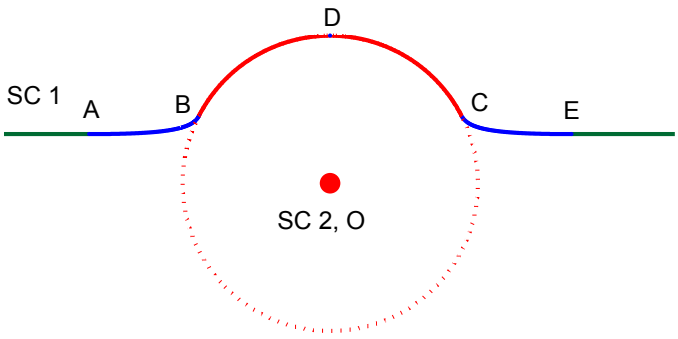

Figure 4 Scenario of the circular Phase II trajectory.

For the following numerical simulations, let the spacecraft have the same mass

$$m_1 = m_2 = 50\text{kg} \tag{48}$$

while the maximum charge product between the two craft is

$$Q_{\max} = 2.5 \times 10^{-11}\text{C}^2 \tag{49}$$

The potential collision range r_o and the safe-restraint distance r_s are

$$r_o = 10\text{m}, \quad r_s = 5\text{m} \tag{50}$$

The initial inertial positions and velocities of the two spacecraft are chosen as

$$\begin{cases} \boldsymbol{R}_1(t_0) = [0,0,0]^T\text{m} \\ \boldsymbol{R}_2(t_0) = [14,2,0]^T\text{m} \end{cases} \qquad \begin{cases} \dot{\boldsymbol{R}}_1(t_0) = [0,0,0]^T\text{m/s} \\ \dot{\boldsymbol{R}}_2(t_0) = [-0.04,0,0]^T\text{m/s} \end{cases} \tag{51}$$

The multiplier in Eq. (11) is set to be $\gamma = 1$, which means after the iteration routine converges, $r_{p\text{II}} = r_s$ and the closest distance in the entire trajectory is r_s. The analytical solution to Eq. (35) is chosen to be

$$\mu_{\text{II}} = \frac{-l_2 - \sqrt{l_2^2 - 4l_1l_3}}{2l_1} \tag{52}$$

Figure 5 shows the numerical search results. Figure 5(a) illustrates the relative trajectory as seen by SC1. In this simulation, the iteration routine ends up with $r_{p\text{II}} = r_s = 5\text{m}$, and the radius of the apoapsis is $r_{a\text{II}} = 8.7808\text{m}$. The final direction of the relative motion is the same as the initial relative motion direction which can be seen from Figure 5(a). The magnitude of the final departure relative velocity converges to the initial relative velocity magnitude as shown in Figure 5(d). And Figure 5(e) shows that the velocity direction also converges to the initial heading direction. These results match up with the intention of the symmetric patched conic section programming.

Figure 5(b) is the history of the charge product Q. In Phase I and Phase III, $Q = Q_{\max} = 25\mu\text{C}^2$ to create two repelling hyperbola. In Phase II, $Q = -2.973\mu\text{C}^2 < 0$, it results in a constant, positive effective gravitational coefficient to form an attracting conic section. The magnitude is less than the limit of the charge product. Figure 5(c) is the trajectories of the two spacecraft as seen in an inertial frame.

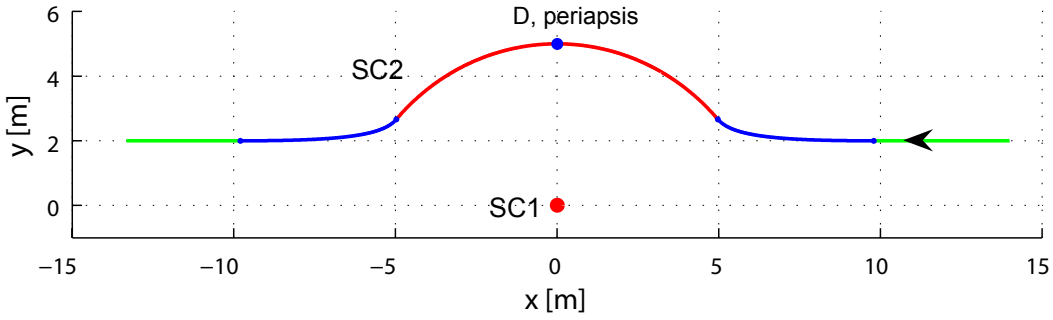

(a) Relative trajectory scenario.

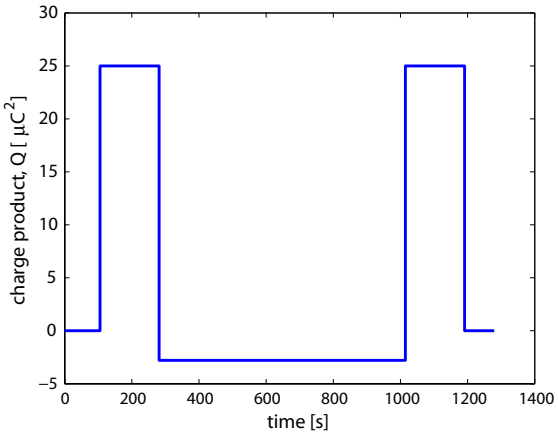

(b) History of the charge product.

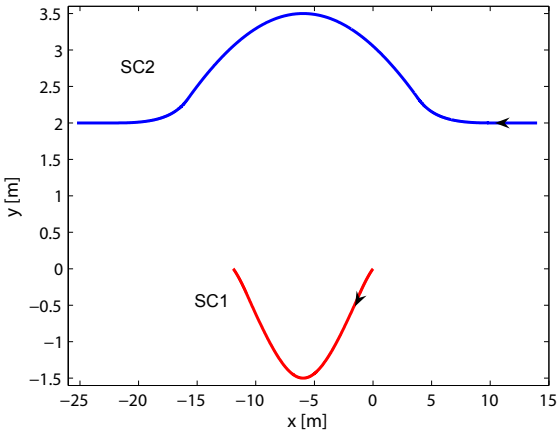

(c) Trajectories of two craft in inertial frame.

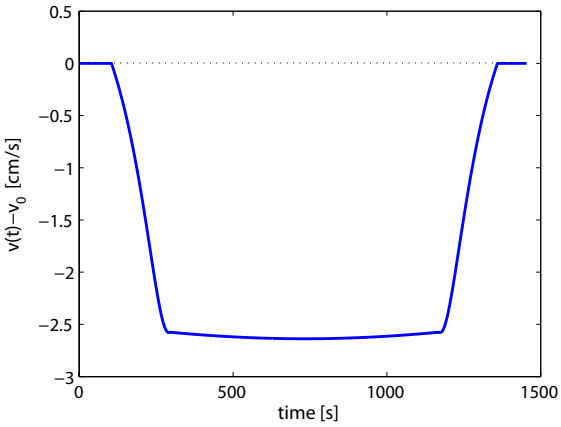

(d) Velocity magnitude error, $\|\dot{\boldsymbol{r}}(t)\| - \|\dot{\boldsymbol{r}}_0\|$.

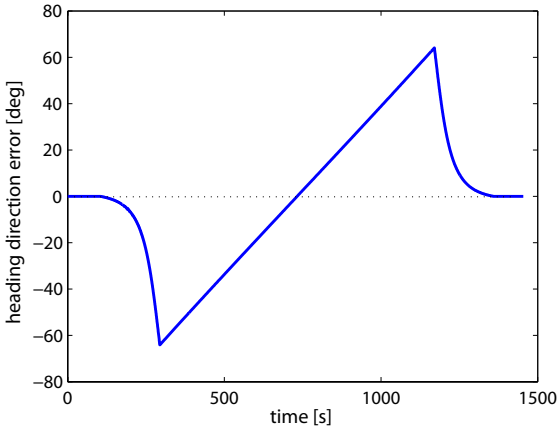

(e) Velocity direction error in angle.

Figure 5 Symmetric patched conic section search results.

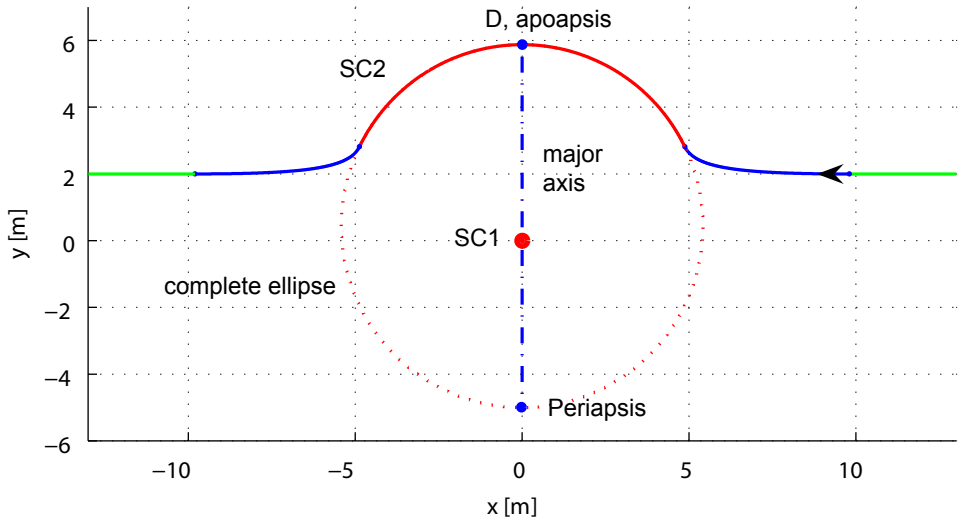

Figure 6 Relative trajectory scenario with D being the apoapsis.

With the same initial conditions and the control parameters, but using the other solution to Eq. (35):

$$\mu_{\text{II}} = \frac{-l_2 + \sqrt{l_2^2 - 4l_1 l_3}}{2l_1} \tag{53}$$

yields a different solution as shown in Figure 6. In this relative trajectory scenario, the point D is the apoapsis of the complete Phase II ellipse. The periapsis radius is $r_{p\text{II}} = 5\text{m}$, and the apoapsis radius is $r_{a\text{II}} = 5.8732\text{m}$. The convergence criteria $r_{p\text{II}} = r_s$ is still satisfied, and the resulting relative trajectory is an expected symmetric patched conic section.

Though the above simulations show perfect results of the numerical search routine, it's not guaranteed that the routine always comes out with an expected solution. Studying Eq. (32) again, it can be found that there are four solutions for $f_{B\text{II}}$ to satisfy Eq. (35), they are:

$$[\angle BOD, \quad \pi - \angle BOD, \quad -\angle BOD, \quad \angle BOD - \pi] \tag{54}$$

We have known that $f_{B\text{II}} = -\angle BOD$ corresponds to the case that the point D is the periapsis, and $f_{B\text{II}} = \pi - \angle BOD$ indicates the point D is the apoapsis of the conic section. Both of these two values of the angle $f_{B\text{II}}$ result in symmetric patched conic section trajectories. But the other two values lead to non-symmetric solutions. These non-symmetric solutions need to be analysed further, and avoided if possible since they will cause the craft to depart at different relative heading angles their their approach trajectories. Another problem needs to be solved is the convergence analysis of the iteration routine. The given technique to determine an initial state guess for the iteration routine works well in many cases, but not all. Further studies will investigate more robust initial condition setup routines.

CONCLUSION

A two spacecraft collision avoidance problem is discussed in this paper. An open-loop trajectory programming algorithm is developed to find a general symmetric patched conic-section relative

trajectory. Compared to previously published feedback charge control strategies to avoid a collision, this approach is able to match both the direction and the magnitude of the relative motion speed with the initial relative approach velocity vector. By assuming the value of the charge product in Phase I to be the maximum charge level the craft can safely attain, five equality constraints are introduced to set up a symmetric three-conic-section trajectory for the five DOF problem. Four constraints are used to formulate the trajectory. Newton's method is used to iteratively search for an appropriate time variable t_B to satisfy the remaining one constraint. Two possible solution for a given set of initial conditions are discussed. Another approach seeking a circular trajectory in Phase II is presented. The circular trajectory constraint adds an additional constraint into the system, thus there exits a unique solution to the five DOF problem without assuming the maximum charge value during Phase I. Future work will investigate determining a minimum charge solution that construct a symmetric trajectory.

REFERENCES

[1] R. P. Patera and G. E. Peterson, "Space Vehicle Maneuver Method to Lower Collision Risk to an Acceptable Level," *Journal of Guidance, Control, and Dynamics*, Vol. 26, March–April 2003, pp. 233–237.

[2] G. L. Slater, S. M. Byram, and T. W. Williams, "Collision Avoidance for Satellites in Formation Flight," *Journal of Guidance, Control, and Dyanmics*, Vol. 29, Sept.-Oct. 2006, pp. 1140–1146.

[3] R. P. Patera, "Space Vehicle Conflict-Avoidance Analysis," *Journal of Guidance, Control, and Dynamics*, Vol. 30, March–April 2007, pp. 492–498.

[4] L. B. King, G. G. Parker, S. Deshmukh, and J.-H. Chong, "Spacecraft Formation-Flying using Inter-Vehicle Coulomb Forces," tech. rep., NASA/NIAC, January 2002. `http://www.niac.usra.edu`.

[5] D. R. Nicholson, *Introduction to Plasma Theory*. Krieger, 1992.

[6] T. I. Gombosi, *Physics of the Space Environment*. Cambridge University Press, 1998.

[7] C. C. Romanelli, A. Natarajan, H. Schaub, G. G. Parker, and L. B. King, "Coulomb Spacecraft Voltage Study Due to Differential Orbital Perturbations," *AAS Space Flight Mechanics Meeting*, Tampa, FL, Jan. 22–26 2006. Paper No. AAS-06-123.

[8] V. Lappas, C. Saaj, D. Richie, M. Peck, B. Streeman, and H. Schaub, "Spacecraft Formation Flying and Reconfiguration with Electrostatic Forces," *AAS/AIAA Space Flight Mechanics Meeting*, Sedona, AZ, Jan. 28–Feb. 1 2007. Paper AAS 07–113.

[9] H. Schaub and I. I. Hussein, "Stability and Reconfiguration Analysis of a Circulary Spinning 2-Craft Coulomb Tether," *IEEE Aerospace Conference*, Big Sky, MT, March 3–10 2007.

[10] H. Vasavada and H. Schaub, "Analytic Solutions for Equal Mass 4-Craft Static Coulomb Formation," *AAS/AIAA Astrodynamics Specialists Conference*, Mackinac Island, MI, Aug. 19–23 2007. Paper AAS 07–268.

[11] S. Wang and H. Schaub, "1-D Constrained Coulomb Structure Stabilization With Charge Saturation," *AAS/AIAA Astrodynamics Specialists Conference*, Mackinac Island, MI, Aug. 19–23 2007. Paper AAS 07–267.

[12] I. I. Hussein and H. Schaub, "Stability and Control of Relative Equilibria for the Three-Spacecraft Coulomb Tether Problem," *AAS/AIAA Astrodynamics Specialists Conference*, Mackinac Island, MI, Aug. 19–23 2007. Paper AAS 07–269.

[13] S. Wang and H. Schaub, "Spacecraft Collision Avoidance Using Coulomb Forces With Separation Distance Feedback," *AAS/AIAA Space Flight Mechanics Meeting*, No. Paper No. AAS 07-112, Sedona, Arizona, January 28–February 1 2007.

[14] I. I. Hussein and H. Schaub, "Invariant Shape Solutions of the Spinning Three Craft Coulomb Tether Problem," *AAS Space Flight Mechanics Meeting*, Tampa, Florida, January 22–26 2006. Paper No. AAS 06-228.

[15] H. Schaub, G. G. Parker, and L. B. King, "Challenges and Prospect of Coulomb Formations," *Journal of the Astronautical Sciences*, Vol. 52, Jan.–June 2004, pp. 169–193.

[16] H. Schaub and J. L. Junkins, *Analytical Mechanics of Space Systems*. Reston, VA: AIAA Education Series, October 2003.